The influence of magnetic fields on the gravitational-wave emission from binary neutron stars

Bruno Giacomazzo,[1] Luciano Rezzolla,[1,2] and Luca Baiotti[3]

[1] *Max-Planck-Institut für Gravitationsphysik, Albert-Einstein-Institut, Potsdam-Golm, Germany*
[2] *Department of Physics and Astronomy, Louisiana State University, Baton Rouge, LA, USA*
[3] *Graduate School of Arts and Sciences, University of Tokyo, Komaba, Meguro-ku, Tokyo, 153-8902, Japan*

(Dated: January 18, 2009)

Using accurate and fully general-relativistic simulations we assess the effect that magnetic fields have on the gravitational-wave emission produced during the inspiral and merger of magnetized neutron stars. In particular, we show that magnetic fields have an impact after the merger, because amplified by a Kelvin-Helmholtz instability, but *also* during the inspiral, because the magnetic tension reduces the stellar tidal deformation for extremely large initial magnetic fields, $B_0 \gtrsim 10^{17}$ G. We quantify the influence of magnetic fields by computing the overlap, $\mathcal{O}$, between the waveforms produced during the inspiral by magnetized and unmagnetized binaries. We find that for $B_0 \simeq 10^{17}$ G, $\mathcal{O} \lesssim 0.76$ for stars with mass $M \simeq 1.4\,M_\odot$, dropping to $\mathcal{O} \lesssim 0.67$ for $M \simeq 1.6\,M_\odot$; in both cases $\mathcal{O}$ decreases further after the merger. These results shed light on the recent debate on whether the presence of magnetic fields can be detected during the inspiral and highlight that the use of higher-order methods is essential to draw robust conclusions on this complex process.

PACS numbers: 04.30.Db, 04.40.Dg, 04.70.Bw, 95.30.Qd, 97.60.Jd

I. Introduction.—Numerous astronomical observations suggest that large magnetic fields (MFs) are associated with neutron stars (NSs). Indeed, evidence for the existence of binary NSs is obtained from binary pulsars, in which one or both NSs are seen to have a large MF. Such binary systems are expected to emit gravitational waves (GWs) strong enough to be relevant for the detectors now operative at design sensitivities. Finally, the coalescence of NSs gives rise, either promptly or after a few seconds, to a system composed of a torus orbiting around a rapidly rotating black hole (BH) [1, 2]. The complex plasma physics accompanying this event is probably behind the "engine" powering short gamma-ray bursts (GRB) [3, 4].

There is little doubt, therefore, about the importance of assessing the role played by MFs in the inspiral and merger of binary NSs. Yet, determining this accurately is a remarkably difficult task requiring the solution of the Einstein equations together with those of general-relativistic magnetohydrodynamics (GRMHD). So far, only two GRMHD simulations have been reported [5, 6], reaching different conclusions about the importance of MFs for the inspiral phase. The aim of this paper is to go beyond these qualitative estimates and provide a first quantitative measurement of the influence of MFs on both the inspiral and the merger of magnetized NSs.

Overall, we find that MFs play a very important role after the merger, when the turbulent motions triggered at the merger by the Kelvin-Helmholtz instability amplify any initial poloidal MF producing a toroidal one, which rapidly becomes comparable to the poloidal one. In addition, we also find that MFs can play a role already during the inspiral if sufficiently strong. This is due to the magnetic tension, which decreases the NS deformability, increases the compactness, and thus delays the time of merger. Finally, our results show that higher-order numerical methods are essential to draw robust conclusions on this process and that, instead, lower-order methods incorrectly suggest that MFs have no influence at all.

II. Mathematical and numerical setup.—All the results presented here were computed by solving the GRMHD equations in the ideal MHD approximation (*i.e.*, assuming an infinite electrical conductivity) and in dynamical spacetimes. More specifically, the evolution of the spacetime was obtained using the `CCATIE` code, a three-dimensional finite-differencing code providing a solution of a conformally traceless formulation of the Einstein equations [7]. The GRMHD equations were instead solved using the `Whisky` code presented in [8], thus adopting a flux-conservative formulation of the GRMHD equations [9] and high-resolution shock-capturing schemes. In particular, we have computed the fluxes using the Harten-Lax-van Leer-Einfeldt (HLLE) approximate Riemann solver [10], while the reconstruction was made using the 3rd-order PPM scheme. Furthermore, to guarantee the divergence-free character of the MHD equations we have employed the flux-constrain-transport approach [11]. The code has been validated against a series of tests in special relativity [12] and in full general relativity (see [8] for a discussion).

The system of GRMHD equations is closed by an equation of state (EOS) and, as discussed in detail in [1], the choice of the EOS plays a fundamental role in the post-merger dynamics and significantly influences the survival time against gravitational collapse of the hyper-massive neutron star (HMNS) likely produced by the merger. It is therefore important that special attention is paid to use EOSs that are physically realistic, as done in [13] within a conformally description of the fields and a simplified treatment of the hydrodynamics. Because we are here mostly concerned with computing a first quantitative estimate of the role played by MFs rather than with a realistic description of the NS matter, we have employed the commonly used "ideal-fluid" EOS in which the pressure p is expressed as $p = \rho\,\epsilon(\Gamma - 1)$, where ρ is the rest-mass density, ϵ is the specific internal energy and Γ is the adiabatic exponent. While simple, such EOS provides a reasonable approximation and we expect that the use of realistic EOSs would not change the main results of this work.

TABLE I: Properties of the eight equal-mass binaries considered: proper separation between the stellar centres $d/M_{\rm ADM}$; baryon mass M_b of each star; total ADM mass $M_{\rm ADM}$; angular momentum J; initial orbital angular velocity Ω_0; mean coordinate radius r_e along the line connecting the two stars; ratio of the polar to the equatorial coordinate radii r_p/r_e; maximum rest-mass density $\rho_{\rm max}$; maximum initial MF B_0, where $*$ is either 0 (in which case $B_0 = 0$), 12, 14 or 17. Note that $M_{\rm ADM}$ and J are reported as measured on the finite-difference grid.

Binary	$d/M_{\rm ADM}$	$M_b\ (M_\odot)$	$M_{\rm ADM}\ (M_\odot)$	$J\ ({\rm g\,cm^2/s})$	$\Omega_0\ ({\rm rad/ms})$	$r_e\ ({\rm km})$	r_p/r_e	$\rho_{\rm max}\ ({\rm gm/cm^3})$	$B_0\ ({\rm G})$
M1.45-B$*$	14.3	1.445	2.681	6.5083×10^{49}	1.78	15.2 ± 0.3	0.899	4.58×10^{14}	0 or $1.97\times10^{*}$
M1.62-B$*$	13.2	1.625	2.982	7.7805×10^{49}	1.85	13.7 ± 0.3	0.931	5.91×10^{14}	0 or $1.97\times10^{*}$

Both the Einstein and the MHD equations are solved using the vertex-centered mesh-refinement scheme provided by the `Carpet` driver [14]. An important difference with respect to [1] is that we have here used fixed mesh refinements rather than moving ones. While computationally more expensive, this choice reduces the violations in the divergence of the MF due to interpolations in the buffer zones between refinement levels. In this way, the divergence of the MF on the finest grid (not including the buffer zones) is zero at machine precision.

We have used five refinement levels with π and equatorial symmetry, the finest one having a resolution of $h = 354.4\,{\rm m}$ and extending up to $r = 44\,{\rm km}$ while the coarsest grid has a resolution of $h = 5.6704\,{\rm km}$ and it extends up to $r = 380\,{\rm km}$. Our finest grid therefore contains both NSs at all times and each NS is covered with $\approx 80^3$ points. Note that in [5] the finest grid had $h = 0.46\,{\rm km}$, thus with $\approx 70^3$ points across each star, while these were $\gtrsim 40^3$ in [6]. Although our resolution is half of that in [1], but higher than that in [5, 6], it is barely sufficient to reach convergent results for the inspiral.

III. Initial data.—The initial data are the same used in [1] and were produced by Taniguchi and Gourgoulhon [15] with the multi-domain spectral-method code `LORENE` [16]. The initial solutions for the binaries are obtained assuming a quasi-circular orbit, an irrotational velocity field, and a conformally-flat spatial metric. The matter is modelled using a polytropic EOS $p = K\rho^\Gamma$ with $K = 123.6$ and $\Gamma = 2$. Since no self-consistent solution is yet available for magnetized binaries, a poloidal MF is added a-posteriori using the vector potential

$$A_\phi \equiv \varpi^2 A_b \max\left(P - P_{\rm cut}, 0\right)^{n_{\rm s}}\,, \qquad (1)$$

where $\varpi \equiv \sqrt{x^2+y^2}$, $A_b > 0$ parameterizes the strength of the MF, $P_{\rm cut}$ defines where in the NS the MF goes to zero, and $n_{\rm s}$ determines the smoothness of the potential. The components of the MF are then computed by taking the curl of the Cartesian components of (1) to enforce that the divergence of the MF is zero at machine precision. Here we have set $P_{\rm cut} = 0.04\max(P)$, and $n_{\rm s} = 2$ to enforce that both the MF and its first derivative are zero at $P = P_{\rm cut}$. In [5] the MF was built with an equivalent expression but with $P_{\rm cut}$ set to the pressure in the atmosphere, and in [6] the expression used is only slightly different, but $P_{\rm cut}$ is set to be $4\% - 0.1\%$ of $\max(P)$. In both [5] and [6] $n_{\rm s} = 1$. Note that the MFs are confined at all times inside the NS matter and hence they cannot "repel" each other during the inspiral, as claimed in [5].

Table I lists some of the properties of the eight equal-mass binaries considered here. More specifically, we have considered two classes of binaries differing in the initial masses, *i.e.,* binaries M1.45-B$*$ (or low-mass), and binaries M1.62-B$*$ (or high-mass). For each of these classes we have considered four different magnetizations (indicated by the asterisk) so that, for instance, M1.45-B12 is a low-mass binary with a maximum initial MF $B_0 = 1.97\times10^{12}\,{\rm G}$. Note that the binaries with zero MFs are the same as those evolved in [1] and that we consider binaries with $B_0 \simeq 10^{17}\,{\rm G}$ not because realistic but because they provide useful upper limits.

IV. GWs and overlaps.—We postpone the discussion on the matter dynamics to a subsequent paper and concentrate here on the GW emission. A representative summary is offered in Fig. 1, which reports the $\ell = 2, m = 2$ component of the h_+ polarization (modulo a phase difference $h_\times$ shows the same behaviour). More specifically, Fig. 1 highlights the differences in the GWs from binaries with different masses, *i.e.,* $1.62\,M_\odot$ (solid line) and $1.45\,M_\odot$ (dashed line) when the initial MF is either zero (top panel) or when it is as high as $\simeq 10^{17}\,{\rm G}$ (bottom panel). Figure 1 clearly shows that when the NSs are not magnetized, the high-mass binary has a larger-amplitude GW emission, it experiences an earlier merger and the HMNS at these resolutions collapses to a rapidly rotating BH after only $\sim 4\,{\rm ms}$, while the HMNS from the low-mass binary does not collapse. In contrast, when the NSs are initially magnetized, the strong magnetic tension reduces the tidal deformations and results in a delayed merger time [18]. Furthermore, the additional pressure support coming from the intense MFs is such that neither the high-mass nor the low-mass binary collapse promptly to a BH over the $\sim 15\,{\rm ms}$ of the simulations (see the bottom panel of Fig. 4 for a comparison of GWs for high-mass binaries with different MFs). Overall, Fig. 1 shows that MFs have a strong impact on the GWs emitted after the merger but *also* during the inspiral, if sufficiently strong. Note again that the delayed merger is not due to the interaction between the dipolar MFs (*cf.* [5]) but is instead produced by the increased stellar compactness.

While generic, this behaviour depends sensitively on the strength of the initial MF and there exists a critical MF below which the MHD effects during the inspiral are not important. We have therefore computed the overlap between two waveforms $h_{\rm B1},\ h_{\rm B2}$ from binaries with initial MFs B1, B2 as

$$\mathcal{O}[h_{\rm B1}, h_{\rm B2}] \equiv \frac{\langle h_{\rm B1}|h_{\rm B2}\rangle}{\sqrt{\langle h_{\rm B1}|h_{\rm B1}\rangle\langle h_{\rm B2}|h_{\rm B2}\rangle}}\,, \qquad (2)$$

where $\langle h_{\rm B1}|h_{\rm B2}\rangle$ is the scalar product and is defined as

$$\langle h_{\rm B1}|h_{\rm B2}\rangle \equiv 4\Re\int_0^\infty df\,\frac{\tilde h_{\rm B1}(f)\tilde h^*_{\rm B2}(f)}{S_h(f)}\,, \qquad (3)$$

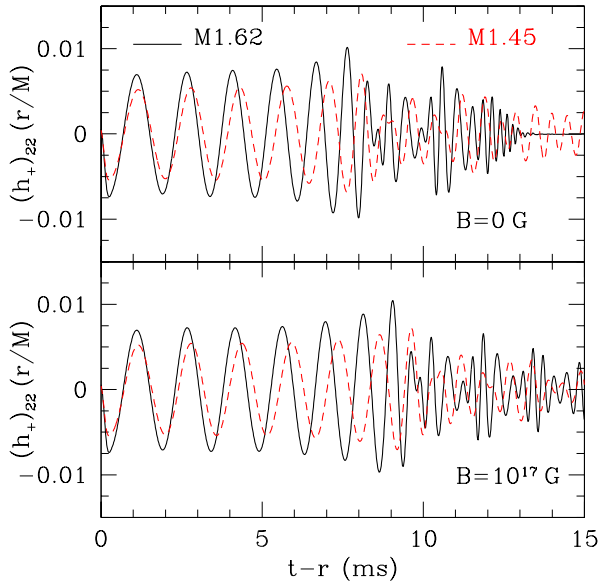

FIG. 1: *Top panel:* $\ell = 2$, $m = 2$ component of the h_+ polarization from binaries with different masses *i.e.,* $1.62\,M_\odot$ (solid line) and $1.45\,M_\odot$ (dashed line) and zero MF. *Bottom panel:* the same as in the top panel but for binaries with an initial MF $B_0 \simeq 10^{17}$ G.

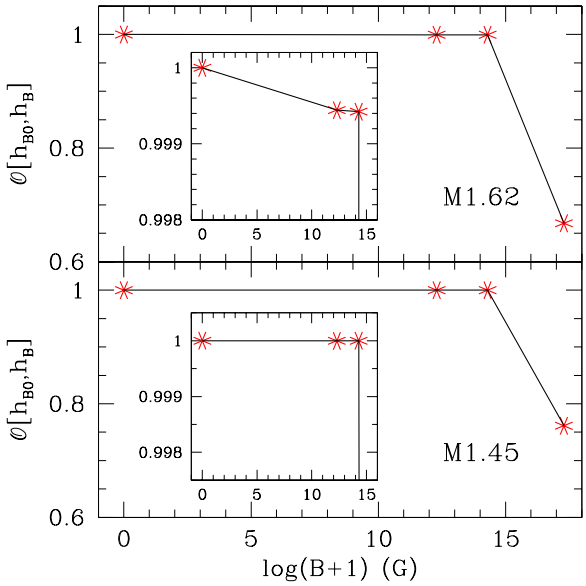

FIG. 2: Overlap in inspiral waveforms from binaries with different magnetizations and the unmagnetized ones; the top and bottom panels refer to the high- and low-mass binaries, respectively.

and $\tilde{h}(f)$ is the Fourier transform of the GW $h(t)$ and $S_h(f)$ is the noise power spectral density of the detector (we have here considered LIGO). Clearly, waveforms that are very similar have $\mathcal{O} \simeq 1$, and a general view is shown in Fig. 2, which reports the overlaps between the unmagnetized binaries and binaries with different magnetizations, *i.e.,* $\mathcal{O}[h_{\rm B0}, h_{\rm B}]$, for the two masses considered here (top and bottom panels, respectively). Note that the overlap is relative to the inspiral only [*i.e.,* the integral (3) is cut off at the orbital frequency at merger] since this is the phase for which our results are convergent (becoming only consistent after the merger as a result of the development of turbulence) and because the post-merger evolution can only further decrease $\mathcal{O}$. It is evident that for the high-mass binary (top panel) the influence of the MF is noticeable only for very large MFs, with $\mathcal{O} \simeq 0.999$ for $B_0 \simeq 10^{14}$ G, which however drops to $\mathcal{O} \simeq 0.668$ for $B_0 \simeq 10^{17}$ G. This is true also for the low-mass binary (bottom panel) whose smaller compactness, however, leads to larger overlaps (*i.e.,* $\mathcal{O} \simeq 0.761$ for $B_0 \simeq 10^{17}$ G).

V. MF amplification.—As discussed in detail in [1], at the merger a shear layer develops in the region where the two NSs enter in contact. Across this layer, the tangential components of the velocity are discontinuous and this leads to the development of a Kelvin-Helmholtz (KH) instability and thus to the production of vortices (*cf.* Fig. 16 of [1]). When poloidal MFs are present, this hydrodynamical instability can lead to exponentially growing toroidal MFs, thus increasing the energy stored in MFs. This mechanism has already been observed in Newtonian simulations [17] and is likely to be important for explaining the physics powering short GRBs. Taking M1.62-B12 as a reference, Fig. 3 shows the evolution of the maxima of the MF $|B| \equiv (B^i B_i)^{1/2}$ (solid line), and of its toroidal $|B^{\rm T}|$ (dashed line), and poloidal $|B^{\rm P}|$ (dot-dashed line) components. A vertical dotted line marks the merger, occurring ≈ 1 ms after the KH instability has started developing. Clearly, as long as the KH instability is active, the toroidal MF is amplified exponentially, until it reaches values comparable to the poloidal one. Note that the MF grows considerably also when the HMNS collapses to a BH as a result of magnetic-flux conservation in the collapsing NS matter.

As discussed in [1, 17], much in the development of the KH instability and in the subsequent MF amplification depends on the resolution used. A detailed study of the turbulent regime and MF amplification produced by the merger is extremely challenging and requires resolutions well above the ones that can be afforded now in GRMHD simulations. Nevertheless, we expect the behaviour in Fig. 3 to be qualitatively correct and, hence, that as long as the KH is active, the poloidal MF is coiled into a toroidal one, increasing it exponentially to values comparable with the poloidal one. When equipartition is reached, the large magnetic tension suppresses the KH instability, preventing a further growth of the toroidal MF. An analysis of this process will be presented elsewhere.

VI. The importance of high-order methods.—As shown in [1], the use of a reconstruction scheme of sufficiently high order is *essential* for a correct calculation of the GW signal. This is highlighted here in Fig. 4, which presents a comparison in the GW emission from the same high-mass binary for evolutions made using either a 2nd-order MINMOD scheme (top panel) or a 3rd-order PPM one (bottom panel). In both cases a solid line refers to the unmagnetized binary while a dashed line to the binary with $B_0 \simeq 10^{17}$ G. Quite clearly, the evolu-

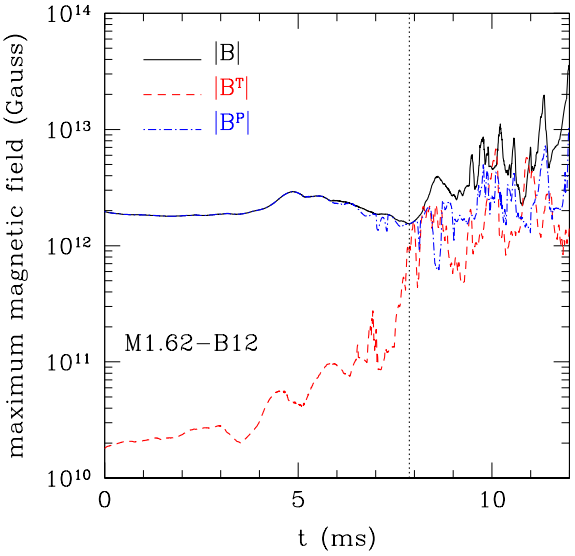

FIG. 3: Evolution of the maxima of the MF $|B| \equiv (B^i B_i)^{1/2}$ (solid line) and of its toroidal $|B^{\rm T}|$ (dashed line) and poloidal $|B^{\rm P}|$ (dot-dashed line) components for the high-mass case with $B_0 \simeq 10^{12}\,{\rm G}$. The vertical dotted line denotes the time of merger.

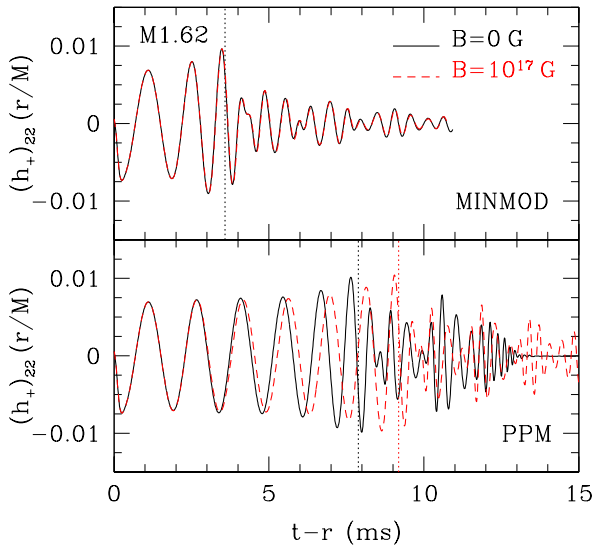

FIG. 4: GW emission from the same high-mass binary evolved using either a 2nd-order scheme (top panel) or a 3rd-order one (bottom panel). A solid (dashed) line refers to a binary with $B_0 = 0\,{\rm G}$ (10^{17} G), while the vertical dotted lines indicate the time of merger.

tions with MINMOD show only minimal differences between the magnetized and unmagnetized case ($\mathcal{O} = 0.9994$ over the whole waveform). In contrast, the evolutions using PPM show considerable differences ($\mathcal{O} = 0.6500$), that are present both during the inspiral and after the merger. More precisely, the binaries evolved with MINMOD merge almost two orbits earlier than those evolved with PPM (*cf.* vertical dotted lines in Fig. 4). Similarly, even the unmagnetized binary evolved with MINMOD does not collapse to a BH, in contrast to what happens when using PPM at these resolutions. These differences are due to the numerical dissipation of the 2nd-order method, which is inadequate at these resolutions. While the truncation error depends on several factors, these results could explain why the calculations in [6], where a 2nd-order reconstruction and a lower resolution was used, show only small differences between unmagnetized and magnetized binaries, and why the merger there occurs in less than one orbit despite the binaries have initial separations comparable to ours.

VII. Conclusions.—We have presented accurate simulations of the inspiral and merger of magnetized NSs and found that MFs have an impact *both* during the inspiral and after the merger. Using the overlap to quantify these differences, we have found that for the inspiral it can be as small as $\mathcal{O} \lesssim 0.67$ for $B_0 \gtrsim 10^{17}\,{\rm G}$; this is produced by the magnetic tension, which reduces the tidal deformation of the NSs before they merge. We have also shown that a KH instability developing at the merger leads to very strong toroidal MFs which modify the structure of the HMNS and further decrease $\mathcal{O}$ after the merger. Finally, we have shown that high-order methods and high resolution are *essential* to draw robust conclusions.

We thank the developers of `Lorene` for providing us with initial data and those of `Carpet` for the mesh refinement. Useful input from C. Palenzuela, D. Neilsen, J. Read, C. Reisswig, E. Schnetter, A. Tonita, and S. Yoshida is also acknowledged. The computations were performed at the AEI and at LONI (`www.loni.org`). This work is also supported by the DFG SFB/Transregio 7 and by the JSPS grant 19-07803.

[1] L. Baiotti, B. Giacomazzo, and L. Rezzolla, Phys. Rev. D **78**, 084033 (2008).
[2] T. Yamamoto, M. Shibata, and K. Taniguchi, Phys. Rev. D **78**, 064054 (2008).
[3] P. Meszaros, Rept. Prog. Phys. **69**, 2259 (2006).
[4] T. Piran, Rev. Mod. Phys. **76**, 1143 (2004).
[5] M. Anderson, et al., Phys. Rev. Lett. **100**, 191101 (2008).
[6] Y. T. Liu, S. L. Shapiro, Z. B. Etienne, and K. Taniguchi, Phys. Rev. D **78**, 024012 (2008).
[7] D. Pollney, et al., Phys. Rev. D **76**, 124002 (2007).
[8] B. Giacomazzo and L. Rezzolla, Class. Quantum Grav. **24**, S235 (2007).
[9] L. Antón, et al., Astrophys. J. **637**, 296 (2006).
[10] A. Harten, P. D. Lax, and B. van Leer, SIAM Rev. **25**, 35 (1983).
[11] G. Toth, J. Comput. Phys. **161**, 605 (2000)
[12] B. Giacomazzo and L. Rezzolla, J. Fluid Mech. **562**, 223 (2006)
[13] R. Oechslin and H. T. Janka, Phys.Rev.Lett. **99**, 121102 (2007)
[14] E. Schnetter, S. H. Hawley, and I. Hawke, Class. Quantum Grav. **21**, 1465 (2004)
[15] K. Taniguchi and E. Gourgoulhon, Phys. Rev. D **66**, 104019 (2002)
[16] URL `http://www.lorene.obspm.fr`.
[17] R. H. Price and S. Rosswog, Science **312**, 719 (2006)
[18] We define the merger as the time when the maximum rest-mass density has a first significant minimum; *cf.* Figs 2 or 8 in [1].